# Document made available under the Patent Cooperation Treaty (PCT)

International application number: PCT/CA05/000032

International filing date: 12 January 2005 (12.01.2005)

Document type: Certified copy of priority document

Document details: Country/Office: US
Number: 60/535,825
Filing date: 13 January 2004 (13.01.2004)

Date of receipt at the International Bureau: 13 April 2005 (13.04.2005)

Remark: Priority document submitted or transmitted to the International Bureau in compliance with Rule 17.1(a) or (b)

PCT/CA 05000032

PA 1285047

# THE UNITED STATES OF AMERICA

## TO ALL TO WHOM THESE PRESENTS SHALL COME:

**UNITED STATES DEPARTMENT OF COMMERCE**

**United States Patent and Trademark Office**

**February 17, 2005**

**THIS IS TO CERTIFY THAT ANNEXED HERETO IS A TRUE COPY FROM THE RECORDS OF THE UNITED STATES PATENT AND TRADEMARK OFFICE OF THOSE PAPERS OF THE BELOW IDENTIFIED PATENT APPLICATION THAT MET THE REQUIREMENTS TO BE GRANTED A FILING DATE UNDER 35 USC 111.**

**APPLICATION NUMBER:** *60/535,825*
**FILING DATE:** *January 13, 2004*

**By Authority of the**
**COMMISSIONER OF PATENTS AND TRADEMARKS**

**W. MONTGOMERY**
**Certifying Officer**

PTO/SB/16 (10-01)
Approved for use through10/31/2002. OMB 0651-0032
U.S. Patent and Trademark Office; U.S. DEPARTMENT OF COMMERCE




# PROVISIONAL APPLICATION FOR PATENT COVER SHEET

This is a request for filing a PROVISIONAL APPLICATION FOR PATENT under 37 CFR 1.53(c).

Express Mail Label No.

## INVENTOR(S)

| Given Name (first and middle [if any]) | Family Name or Surname | Residence (City and either State or Foreign Country) |
|---|---|---|
| Lori | Gardi | London, Ontario, Canada |
| Donal | Downey | London, Ontario, Canada |
| Aaron | Fenster | London, Ontario, Canada |

☐ *Additional inventors are being named on the _____ separately numbered sheets attached hereto*

## TITLE OF THE INVENTION (500 characters max)

Needle Detection, Segmentation and Tracking for 3D Ultrasound-Guided Interventional Procedures

*Direct all correspondence to:* **CORRESPONDENCE ADDRESS**

☐ Customer Number _____ → *Place Customer Number Bar Code Label here*

OR *Type Customer Number here*

| | | | | | |
|---|---|---|---|---|---|
| ☒ Firm or Individual Name | Michael F. Crowley | | | | |
| Address | Robarts Research Institute | | | | |
| Address | P.O. Box 5015, 100 Perth Drive | | | | |
| City | London | State | Ontario | ZIP | |
| Country | Canada | Telephone | (519) 663-3047 | Fax | (519) 663-3173 |

## ENCLOSED APPLICATION PARTS *(check all that apply)*

☒ Specification *Number of Pages* 7
☒ Drawing(s) *Number of Sheets* 12
☐ Application Data Sheet. See 37 CFR 1.76
☐ CD(s), Number
☐ Other (specify)

## METHOD OF PAYMENT OF FILING FEES FOR THIS PROVISIONAL APPLICATION FOR PATENT

☒ Applicant claims small entity status. See 37 CFR 1.27.
☒ A check or money order is enclosed to cover the filing fees
☐ The Commissioner is hereby authorized to charge filing fees or credit any overpayment to Deposit Account Number: _____
☐ Payment by credit card. Form PTO-2038 is attached.

FILING FEE AMOUNT ($): 80

The invention was made by an agency of the United States Government or under a contract with an agency of the United States Government.

☐ No.
☐ Yes, the name of the U.S. Government agency and the Government contract number are: _____

*Respectfully submitted,*

SIGNATURE Michael Crowley

TYPED or PRINTED NAME Michael F. Crowley

TELEPHONE (519) 663-3047

Date Jan. 12, 2004

REGISTRATION NO. *(if appropriate)*

Docket Number:

## USE ONLY FOR FILING A PROVISIONAL APPLICATION FOR PATENT

This collection of information is required by 37 CFR 1.51. The information is used by the public to file (and by the PTO to process) a provisional application. Confidentiality is governed by 35 U.S.C. 122 and 37 CFR 1.14. This collection is estimated to take 8 hours to complete, including gathering, preparing, and submitting the complete provisional application to the PTO. Time will vary depending upon the individual case. Any comments on the amount of time you require to complete this form and/or suggestions for reducing this burden, should be sent to the Chief Information Officer, U.S. Patent and Trademark Office, U.S. Department of Commerce, Washington, D.C. 20231. DO NOT SEND FEES OR COMPLETED FORMS TO THIS ADDRESS. SEND TO: Box Provisional Application, Assistant Commissioner for Patents, Washington, D.C. 20231.

# *PROVISIONAL APPLICATION COVER SHEET*
*Additional Page*

PTO/SB/16 (10-01)
Approved for use through 10/31/2002. OMB 0651-0032
U.S. Patent and Trademark Office; U.S. DEPARTMENT OF COMMERCE


| Docket Number | |
|---|---|

| INVENTOR(S)/APPLICANT(S) | | |
|---|---|---|
| Given Name (first and middle [if any]) | Family or Surname | Residence (City and either State or Foreign Country) |
| | | |

Number _____ of _____

**WARNING: Information on this form may become public. Credit card information should not be included on this form. Provide credit card information and authorization on PTO-2038.**

# NEEDLE DETECTION, SEGMENTATION AND TRACKING FOR 3D ULTRASOUND-GUIDED INTERVENTIONAL PROCEDURES

*Lori Gardi, Donal B. Downey, Aaron Fenster*
*Robarts Research Institute*
*100 Perth Drive, London, ON, CANADA*

## ABSTRACT

Ultrasound-guided interventional procedures such as breast biopsy and prostate brachytherapy require that needles inserted into the body be tracked in near real-time. In robotic-aided interventional procedures such as robot-aided and ultrasound-guided prostate brachytherapy as well as free-hand ultrasound guided biopsy procedures, needles are inserted free from parallel trajectory constraints, i.e., needle trajectories can be positioned with considerable flexibility including oblique trajectories. However, oblique insertion results in the needle intersecting the 2D TRUS image and appearing as a dot, leading to blind guidance. Here, we describe a method for oblique and parallel needle segmentation and tracking to be used in 3D ultrasound guided procedures including robot aided prostate brachytherapy. This approach uses near real-time 3D ultrasound (US) to identify, segment, track and display a needle that is within the 2D US plane or obliquely intersects the plane of the 2D US image. This removes the restriction of the needle having to be parallel to the plane of the transducer in current brachytherapy, cryotherapy and biopsy procedures. The algorithm applies a grey-level change detection technique to find the location and orientation of needles from 3D images. Three 2D images containing the needle (oblique sagittal, coronal and transverse planes) are extracted and displayed in near real-time. Testing showed that our algorithm's accuracy in segmenting the 3D needle's orientation is 0.54° for a chicken tissue phantom, and 0.58° for agar phantoms, over a ±15° insertion orientation. The execution time average is 0.13s on a 1.2 GHz computer.

## 1. INTRODUCTION

This invention has a wide range of applications, such as biopsy of the breast and liver and image guided interventions such as brachytherapy, cryotherapy, as well as other procedures that require a needle or needles to be introduced into soft tissues and be positioned accurately and precisely. As an example, we describe the use of this invention in robot-aided 3D US-guided prostate brachytherapy.

Transperineal prostate brachytherapy provides an improved alternative for minimally-invasive treatment of prostate cancer [1]. However, pubic arch interference (PAI) with the implant path occurs in many patients with large prostates and/or a small pelvis. These patients cannot be treated with

current brachytherapy using parallel needle trajectories guided by a fixed template, because the anterior and/or the antero-lateral parts of the prostate are blocked by the pubic bone.

To solve the PAI problems, it would be advantageous to free needle insertions from parallel trajectory constraints, *i.e.*, needle trajectories should be positioned with considerable flexibility including oblique trajectories [2,3]. The oblique trajectory allows patients with PAI to be treated with brachytherapy without first undergoing lengthy hormonal downsizing therapy. In addition, changes in the prostate size during the implantation may require re-optimization of the dose plan. Thus, combining three-dimensional (3D) transrectal ultrasound (TRUS) imaging, dosimetry and oblique needle insertion trajectories can provide the tools needed for dynamic re-optimization of the dose plan during seed implantation procedure by allowing dynamic adjustments of the needle position to target potential "cold spots".

To achieve this goal, we developed a 3D TRUS-guided robot-aided prostate brachytherapy system [4]. In this system, a robot is used as a movable needle guide containing one-hole needle guide template. The position and orientation of the needle can be changed as the robot moves. By unifying the robot, ultrasound (US) transducer and the 3D TRUS image coordinate systems, the position of the template hole can be accurately related to the 3D TRUS image coordinate system, allowing accurate and consistent insertion of the needle via the hole into the targeted position in the prostate along various trajectories including oblique ones.

However, oblique insertion will result in the needle intersecting the two-dimensional (2D) TRUS image plane, thus the needle will only appear as a dot in this image (see Figure 2). Some investigators have developed automatic needle segmentation methods to locate needles for biopsy and therapy [5,6]. However, these methods require that the needle be completely contained in the 2D US image [6].

In this paper, we describe a near real-time method, for automatic identification, segmentation and tracking of needles during oblique insertion even if the needle exits the 2D US image plane. This method can also be used for automatic identification, segmentation and tracking of needles if they completely contained in the 2D US image plane.

## 2. EXAMPLE APPLICATION

### 2.1. 3D TRUS-guided robotic-assisted system (see Figure 1)

The 3D TRUS imaging system used to test the needle segmentation method consists of a PC with a 1.2 *GHz* processor for 3D image acquisition, reconstruction and display, a video frame grabber for video image acquisition, a mover controller module (*MCM*), which controls the rotation of the trans-rectal ultrasound (TRUS) transducer-mover assembly via the serial port of the computer. To produce 3D TRUS images, the *MCM* and motor assembly causes the transducer to rotate about its long axis over about 100° while 2D TRUS images are digitized at 1° intervals by the frame grabber [7]. These acquired images are reconstructed into a 3D image and are available for viewing in real-time as the 2D

images are being acquired. The 3D TRUS image is viewed using 3D visualization software, which includes multi-planar 3D display as well as an extensive set of measurement tools [10-12].

The robot system (see Fig. 1) includes a robotic arm assembly with 6 degrees-of-freedom. The positioning software can control the robot arm to move in terms of world/tool coordinate systems. The world coordinate system is fixed to the ground and the tool coordinate system is fixed to the robot arm. The robot control software has been integrated together with the 3D US visualization software [4,7] so that we can perform precise image-based robot path planning and visualize multiple potential trajectories in the 3D TRUS image coordinate system using a graphical user interface. Figure 1 shows the whole system.

## 2.2. Needle segmentation algorithm

To perform near real-time needle segmentation, capture of two 3D US images is required. Note, that if the needle is contained in a 2D image, then two 2D US images are required, but the procedure is unchanged. The first (pre-scan) 3D image is obtained by scanning the prostate (tissue) before the needle is inserted, and the second (post-scan) is acquired by scanning only the region containing the needle during needle insertion. The second 3D image is compared against the first and the needle position within the post-scan 3D image, including entry point and needle tip location, is determined using the approach described below and the flow chart shown in Fig. 5.

The needle segmentation method can be used for both linear and rotational 3D US scanning approaches [7]. In addition, our segmentation method can be applied equally well to 3D US images reconstructed using the linear scanning geometry, but acquired using rotational 3D scanning geometry such as that used in prostate imaging. Figure 4(a) shows 3D US images acquired and reconstructed using the rotational geometry approach, but Fig. 4(b) was acquired in the rotational approach and reconstructed using a linear scanning 3D geometry [7]. In Fig. 4(a) needles are stretched horizontally in the 3D scanning direction at the center of the image but are more angulated away from the center. In Fig. 4(b), needles are spread horizontally everywhere in the image, which greatly simplifies the identification and processing image voxels that contain the needle.

### *2.2.1. Grey-level threshold value (see Figure 6)*

A grey-level threshold value is used to reduce the number of voxels to be analyzed and to obtain candidate needle voxels. To determine the threshold value, the maximum grey-level value $GL_{max}$ in the post-scan image is first found. The threshold value is determined by:

$$\text{Threshold value} = a \times GL_{max} \qquad (1)$$

where $0 < a < 1$. In our testing, we used $a = 0.5$.

### *2.2.2. Generating 3D difference map(see Figure 7)*

Voxels with a grey-level change that exceed the threshold value between pre-scan and post-scan are assumed to be part of the needle. In our system, a candidate voxel (CV) containing the needle is defined

as a voxel in the difference 3D image between the pre- and post-scans that exceeds a pre-defined threshold:

$$GLC(i,j,k) = postGL(i,j,k) - preGL(i,j,k) \quad (2)$$

where $preGL(i,j,k)$ and $postGL(i,j,k)$ are the grey-level values at voxel location $(i,j,k)$ in both the pre-scan and the post-scan respectively, and $GLC(i,j,k)$ is the grey level change. A collection of these candidate voxels is referred to as the Difference Map (DM), *i.e.*,

$$(i_m, j_m, k_m) \in \text{3D DM} \quad (3)$$

where $GLC(i_m, j_m, k_m) >$ Threshold Value; $m = 1, 2, \ldots, n$; and $n$ is the number of points included in the 3D difference map (see Fig. 9(a)).

*2.2.3. Selecting needle points (See Figure 8)*

In our system, we have the advantage that the 3D image is reconstructed on demand, therefore, we always have access to the original acquired image data. Since the image of the needle is spread horizontally as shown in Fig. 3 (in the 3D scanning direction), we can remove those voxels from our DM that are not connected to other voxels in this direction as follows:

$$(i_m, j_m, k_m) \notin \text{3D DM}$$
$$\text{when } \bigcup_{m=1}^{p} GLC(i_m, j_m, k_m \pm s) < \text{threshold value}$$

where, $s = 1, 2, \ldots, P/2$; and P is the number of voxels surrounding voxel $(i_m, j_m, k_m)$ in $k$-direction. We chose P = 4 in our algorithm. Figure 9(b) is an example of the DM after the spurious voxels have been rejected.

*2.2.4. Finding the needle trajectory (Block 440 in Figure 5 and Figure 10)*

At this stage needle candidates are available. There are a number of means for identifying the needle trajectory from these candidates. For example, the well-known Hough Transform technique [13] or linear regression may be used, as shown in Blocks 444 and 446 of Figure 10.

***Hough Transform approach:*** We have developed a fast implementation of the Hough Transform [14], which we called the Real-Time Hough Transform. Due to the robustness to the addition of extraneous noise, the Hough Transform is one of the most powerful line detection techniques nowadays and has been widely used in different areas. Unfortunately, its high computation needs often prevents it from being applied in real time applications without the help of specially designed hardware. Our fast implementation of the Hough Transform is based on coarse-fine search and the determination of the optimal image resolution. Comparing to conventional techniques, our approach decreases the time for needle segmentation about two orders of magnitude. Experiments with agar phantoms and patient breast biopsy US image sequences showed that our approach can segment the biopsy needle in real-time (i.e. less than 33ms) on an affordable PC computer without the help of specially designed hardware with the angular rms error about and the position rms error about 0.5 mm.

***Linear regression approach:*** An alternative approach is to use linear regression to find the trajectory of the needle (see Figure 10). The voxels in the difference map (DM) can be fit to a line using linear regression analysis. Once the equation of the line (needle) is obtained, the difference map is further processed to remove voxels that are far away (> 5 voxels) from the line and linear regression is performed again with the filtered data. This procedure is repeated until all the voxels in the difference map are within a prescribed range from the regression line. Figure 9(c) is an example of the DM before the final regression calculation. Once the equation of the line/needle is found, the trajectory of the needle is known. The needle entry point is the intersection of needle trajectory and the known entry plane. The needle tip is the farthest needle voxel along the needle trajectory.

*2.2.5. Extracting of the 2D planes containing the needle*

To extract any plane containing the needle, we use the segmented needle entry point, needle tip point and we select a third point within the 3D image to define a specific plane. In this way, we can extract and display oblique saggital, coronal and transverse views with the needle trajectory highlighted (as described in the flow chart of Fig. 3). Figure 11 shows the result of this complete procedure obtained during a patient's prostate cryotherapy procedure, demonstrating that the needle can be tracked as it is being inserted and orthogonal views can be displayed for the user during the insertion procedure.

## 2.3 Evaluation

*2.3.1. Experimental apparatus*

The accuracy and variability of our needle segmentation and tracking technique was tested using images acquired by scanning phantoms. The robot was used to insert a needle at known angles, including oblique trajectories with respect to the TRUS image plane (Fig. 1).

The needle used in these experiments was a typical 18-gauge (1.2*mm* diameter) prostate brachytherapy needle. The US tissue-mimicking phantoms were made of agar, using a recipe developed by Ricky *et al* [8], and chicken breast tissues [9]. TRUS images were obtained using an 8558/S side-firing linear array transducer with a central frequency of 7.5*MHz*, attached to a B-K Medical 2102 Hawk US machine (B-K, Denmark). The 3D TRUS system consisted of a Pentium III personal computer (PC) equipped with a Matrox Meteor II video frame grabber for 30*Hz* video image acquisition.

*2.3.2. Algorithm execution time*

Execution time depends on the 3D scanning angular interval and the extent of the region to be investigated. To evaluate the algorithm's execution time, first we performed the pre-insertion scan, and then inserted the needle. After needle insertion, the phantom was scanned again, and the needle was segmented. A software timer was used to measure the time duration of the segmentation algorithm.

*2.3.3. Accuracy test*

To test the accuracy of the algorithm, we used the robot to guide the needle insertion into the phantom at known angles (Fig. 1). The angulation accuracy of the robot was evaluated to be 0.12° ± 0.07° [4].

First, we used the robot to guide the needle insertion along a trajectory parallel to the transducer, which we call the 0° orientation. Since the needle could be verified by observing the needle in the real-time 2D TRUS image, we assumed that this trajectory was correct. Thus, our oblique trajectory accuracy measurements could be made with respect to the 0° trajectory. The positions of needle tip and entry point were then found for 0° using the algorithm described above. Then, the robot was used to insert the needle at different angles ($\pm 5^{\circ}, \pm 10^{\circ}, \pm 15^{\circ}$) with respect to the 0° insertion trajectory. For each insertion, the positions of needle tip and entry point were found. The corresponding segmented needle vectors through these entry and needle tip points were determined by:

$$\cos\theta_{alg} = \frac{\vec{A} \bullet \vec{B}}{|\vec{A}||\vec{B}|} \tag{4}$$

where $\vec{A}$ is the segmented needle vector for 0° insertion; $\vec{B}$ is the segmented needle vector for the insertion at any other angle; $\theta_{alg}$ is the angle derived from the segmentation algorithm. The accuracy of the algorithm was evaluated by comparing $\theta_{alg}$ with the robot orientation angle $\theta_{rob}$, *i.e.*,

$$\varepsilon_{\theta} = |\theta_{alg} - \theta_{rob}| \tag{5}$$

The accuracy test was repeated with a chicken tissue phantom, and the accuracy was also determined using Eqs. (4) and (5). For the agar phantoms, we performed five groups of tests to evaluate the algorithm execution time and accuracy. Each group consisted of seven insertions, *i.e.*, insertion at 0° and $\pm 5^{\circ}, \pm 10^{\circ}, \pm 15^{\circ}$. The mean error as a function of insertion angle was calculated, thus:

$$\varepsilon(\theta) = \sum_{i=1}^{5} |(\theta_{alg})_i - (\theta_{rob})_i| / 5. \tag{6}$$

## 3. RESULTS AND CONCLUSION

Table 1 shows the evaluation results. In the chicken tissue phantom, the average execution time was 0.13 ±0.01 seconds, and the average angulation error was 0.54° ± 0.16°. In agar phantoms, the average execution time was 0.12 ±0.01 seconds, and the average angulation error was 0.58° ± 0.36°. The results shown in Table 1 also demonstrate that the insertion error does not significantly depend on insertion angle.

In the 3D US images, needle voxels generally have high grey level values. However, due to specular reflection, some background structures may also appear to have high grey level values. This increases the difficulty in automatic needle segmentation in an US image using grey level information directly

[5,6]. Because US images suffer from low contrast, signal loss due to shadowing, refraction and reverberation artifacts, a grey-level change detection technique appears to be quite robust. In addition, since the needle is segmented from a difference map, complex backgrounds are removed.

In conclusion, we developed a grey-level change detection technique and tested its feasibility for near real-time oblique needle segmentation to be used in 3D TRUS guided and robot aided prostate brachytherapy. Our results show that our segmentation algorithm works well in agar and chicken tissue phantoms. In addition, our approach has also been tested during several prostate cryotherapy procedures with excellent results.

## REFERENCES

[1] D. Ash, D.M. Bottomley, B.M. Carey, "Prostate Brachytherapy," *Prostate Cancer and Prostatic Diseases* **1**, pp. 185-188, 1998.

[2] E.M. Messing, J.B.Y. Zhang, D.J. Rubens, R.A. Brasacchio, J.G. Strrang, A. Soni, P.G. Okunieff, Y. Yu, "Intraoperative optimized inverse planning for prostate brachytherapy: Early experience," *Int J Radiat Oncol Biol Phys* **44**, pp. 801-808, 1999.

[3] G. Cheng, H. Liu, L. Liao, Y. Yu, "Dynamic Brachytherapy of the Prostate Under Active Image Guidance," *Proc of MICCAI 2001*, pp. 351-359, 2001

[4] Z. Wei, G. Wan, L. Gardi, G. Mills, D. Downey, A. Fenster, "Robot-Assisted 3D-TRUS Guided Prostate Brachytherapy: System Integration and Validation," *Med Phys*, 2004, in press.

[5] M. Ding, N. Cardinal, A. Fenster, "Automatic needle segmentation in 3D ultrasound images using orthogonal 2D image projections," *Med Phys* **30**, pp. 222-234, 2003

[6] M. Ding, A. Fenster, "A real-time biopsy needle segmentation technique using Hough Transform," *Med Phys* **30**, pp 2222-2233, 2003

[7] A. Fenster, D. Downey, N. Cardinal, "Topic Review: Three-dimensional ultrasound imaging," *Phys Med Biol* **46**, R67-R99, 2001

[8] D.W. Ricky, P.A. Picot, D.C. Christopher, A. Fenster, "A wall-less vessel phantom for Doppler ultrasound studies," *Ultrasound Med Biol*, **21**, pp. 1163-1175, 1995

[9] W.L. Smith, K.J.M. Surry, G.R. Mills, D.B. Downey, A. Fenster, "Three-dimensional ultrasound-guided core needle breast biopsy," *Ultrasound Med Biol* **27**(8), 1025-1034, 2001

[10] A Fenster, S Dunne, T Chan, D Downey, "*Method and System for Constructing and Displaying Three-Dimensional Images*" U.S. Patent No. 5,454,371: October 3, 1995

[11] J Miller, S Tong, A Fenster, D Downey, "*3-Dimensional Ultrasound Imaging System*" U.S. Patent No. 5,562,095: October 8, 1996

[12] A Fenster, S Dunne, J Larsen "*Three Dimensional Imaging System*" U.S. Patent No. 5,964,707: October 12, 1999

[13] R.O.Duda and P.E.Hart, "Use of Hough Transform to Detect Lines and Curves in pictures: Graphics and Image Processing", Communication of ACM **15**, 11-15 (1972)

[14] M.Ding and A. Fenster, "A real time biopsy needle segmentation technique using the Hough Transform" Medical Physics 30(8), 2222-2233, 2003

# BEST AVAILABLE IMAGES

Defective images within this document are accurate representations of the original documents submitted by the applicant.

Defects in the images may include (but are not limited to):

- BLACK BORDERS
- TEXT CUT OFF AT TOP, BOTTOM OR SIDES
- FADED TEXT
- ILLEGIBLE TEXT
- SKEWED/SLANTED IMAGES
- COLORED PHOTOS
- BLACK OR VERY BLACK AND WHITE DARK PHOTOS
- GRAY SCALE DOCUMENTS

## IMAGES ARE BEST AVAILABLE COPY.

**As rescanning documents *will not* correct images, please do not report the images to the Image Problem Mailbox.**

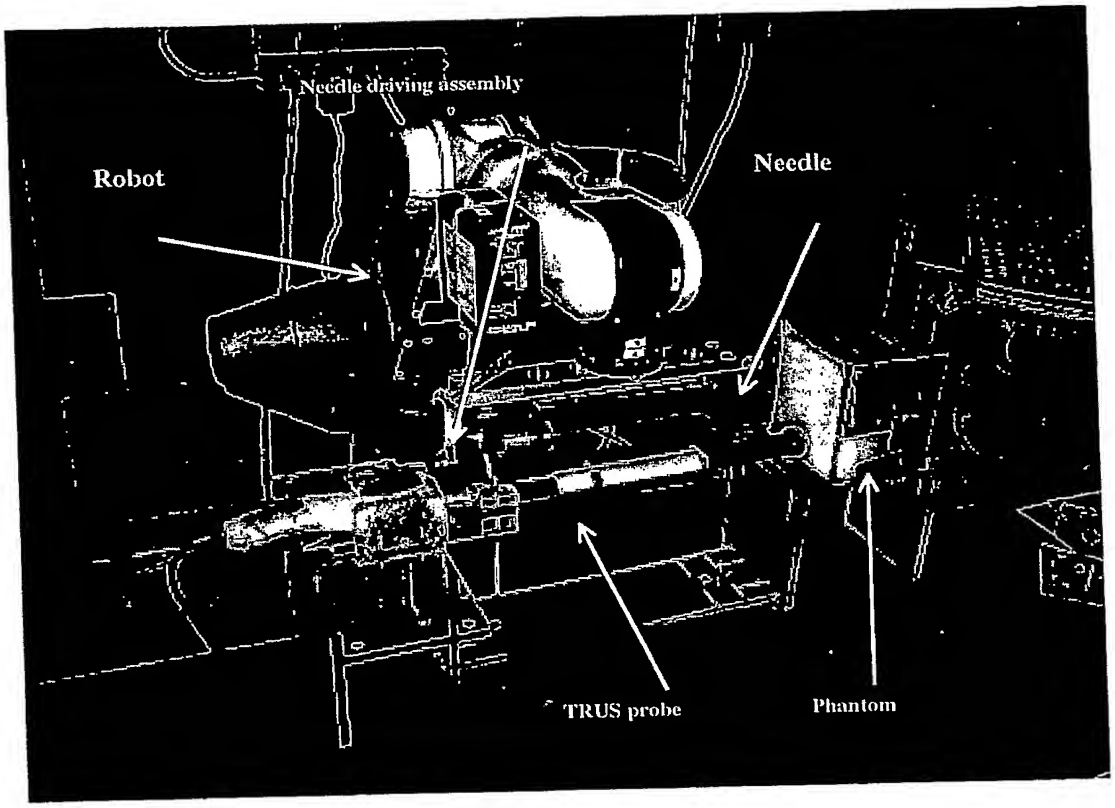


**Figure 1.** 3D TRUS-guided and robot-assisted prostate brachytherapy system.

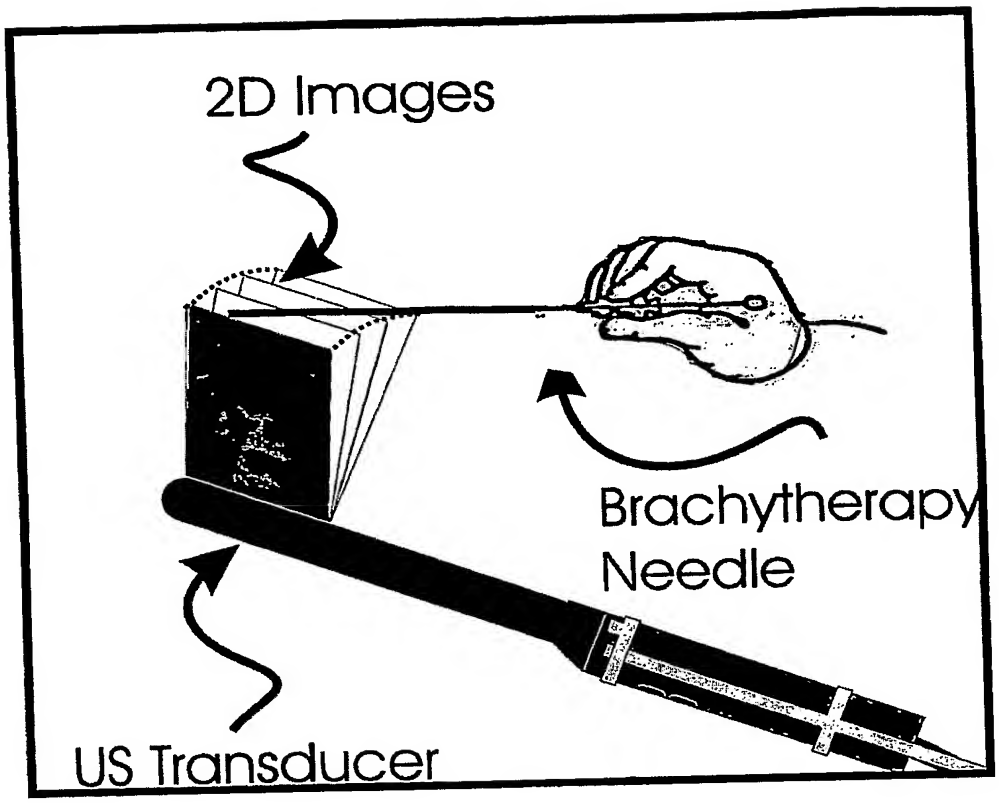


**Figure 2.** Schematic diagram showing the ultrasound transducer mounted on the rotational mover used to produce 3D TRUS images of the prostate. The diagram shows that when the needle is inserted at an oblique angle relative to the transducer's axis, multiple 2D US images are needed to track its insertion trajectory.

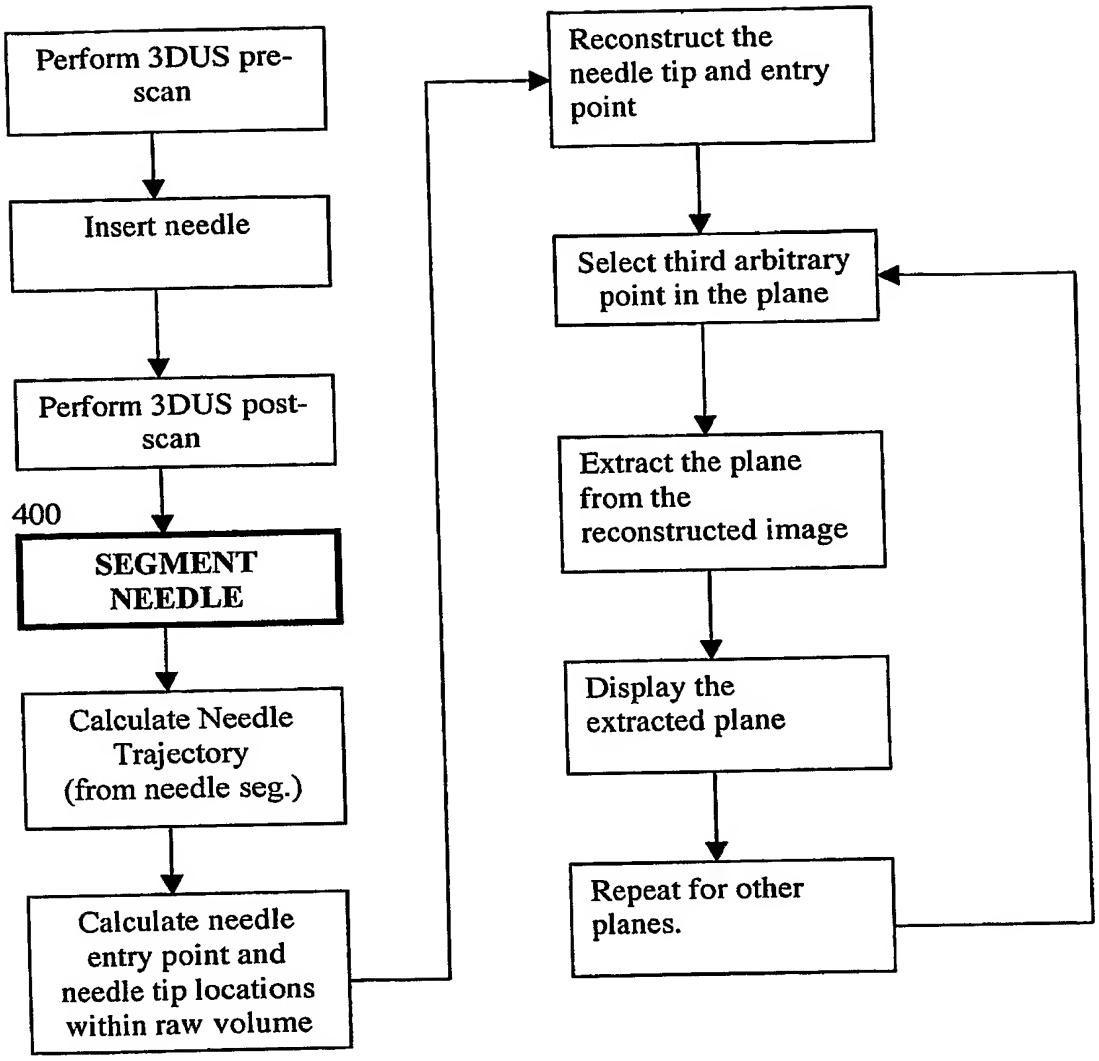


**Figure 3.** Flow chart showing the complete needle identification, segmentation method and display. The step labeled "SEGMENT NEEDLE" is detailed in Figure 5.

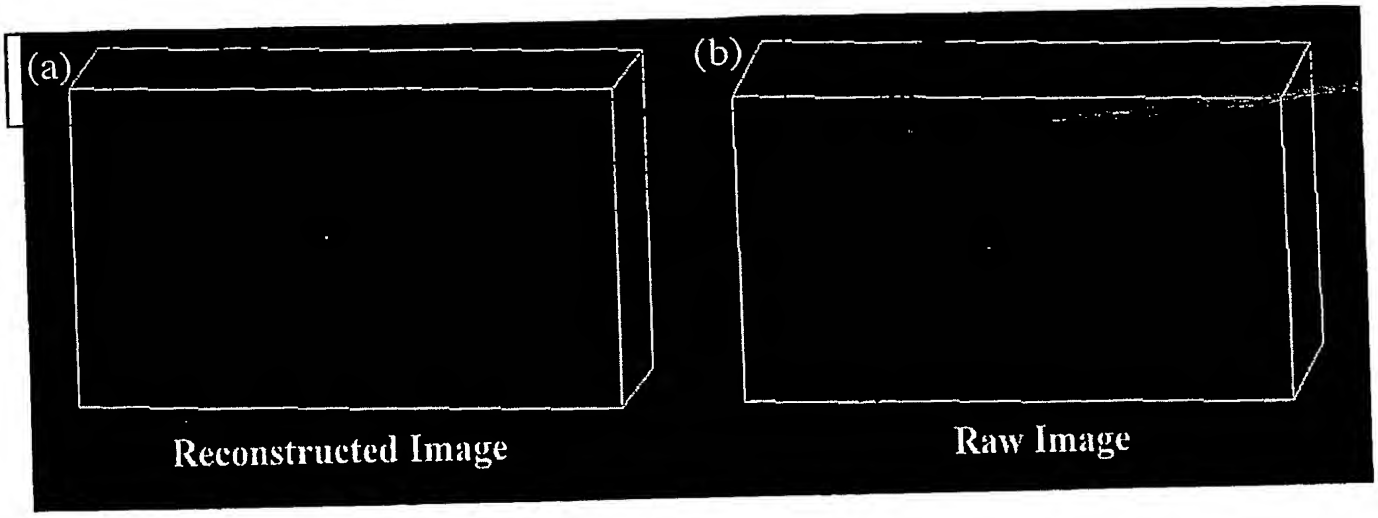


**Figure 4.** The left 3D image has been reconstructed using the proper 3D rotational scanning geometry. The right image has been reconstructed into a 3D image assuming the acquired images are parallel to each other, i.e., without using the rotational scanning geometry.

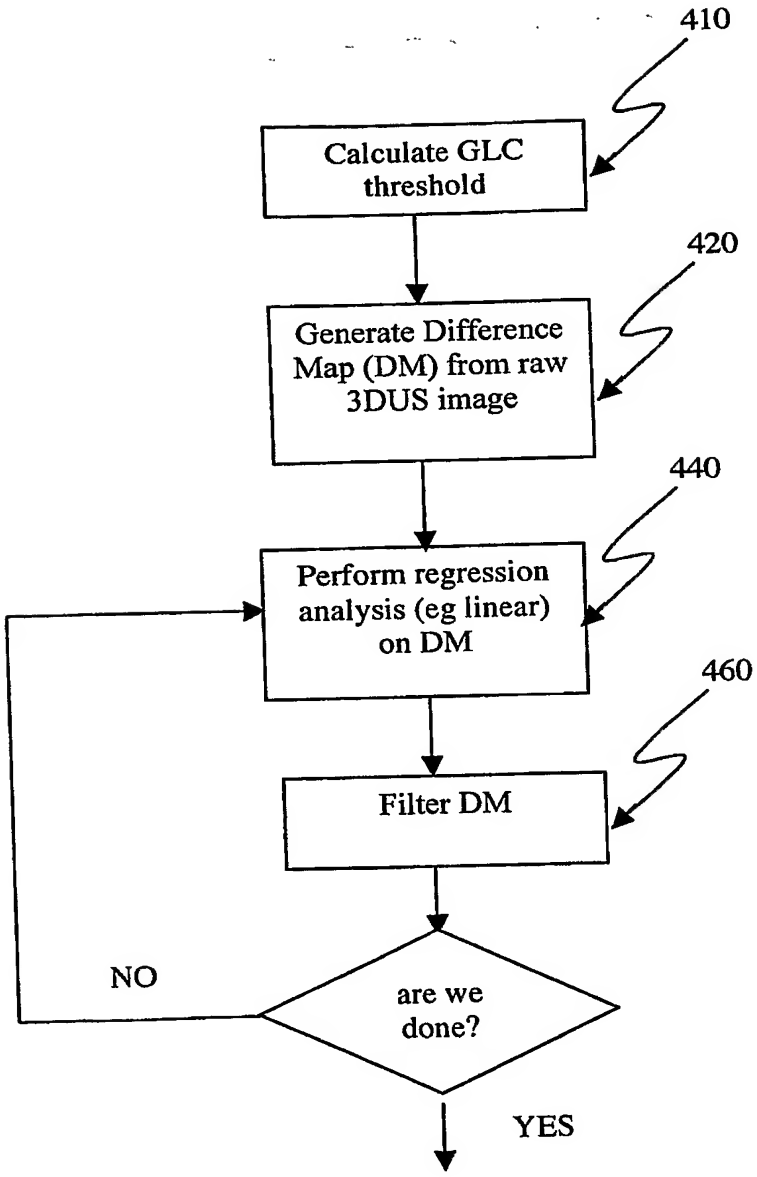


**Figure 5.** Details of Block 400 "SEGMENT NEEDLE" in Fig. 2, i.e. the steps in segmenting the needle using acquired 2D or 3D US images.

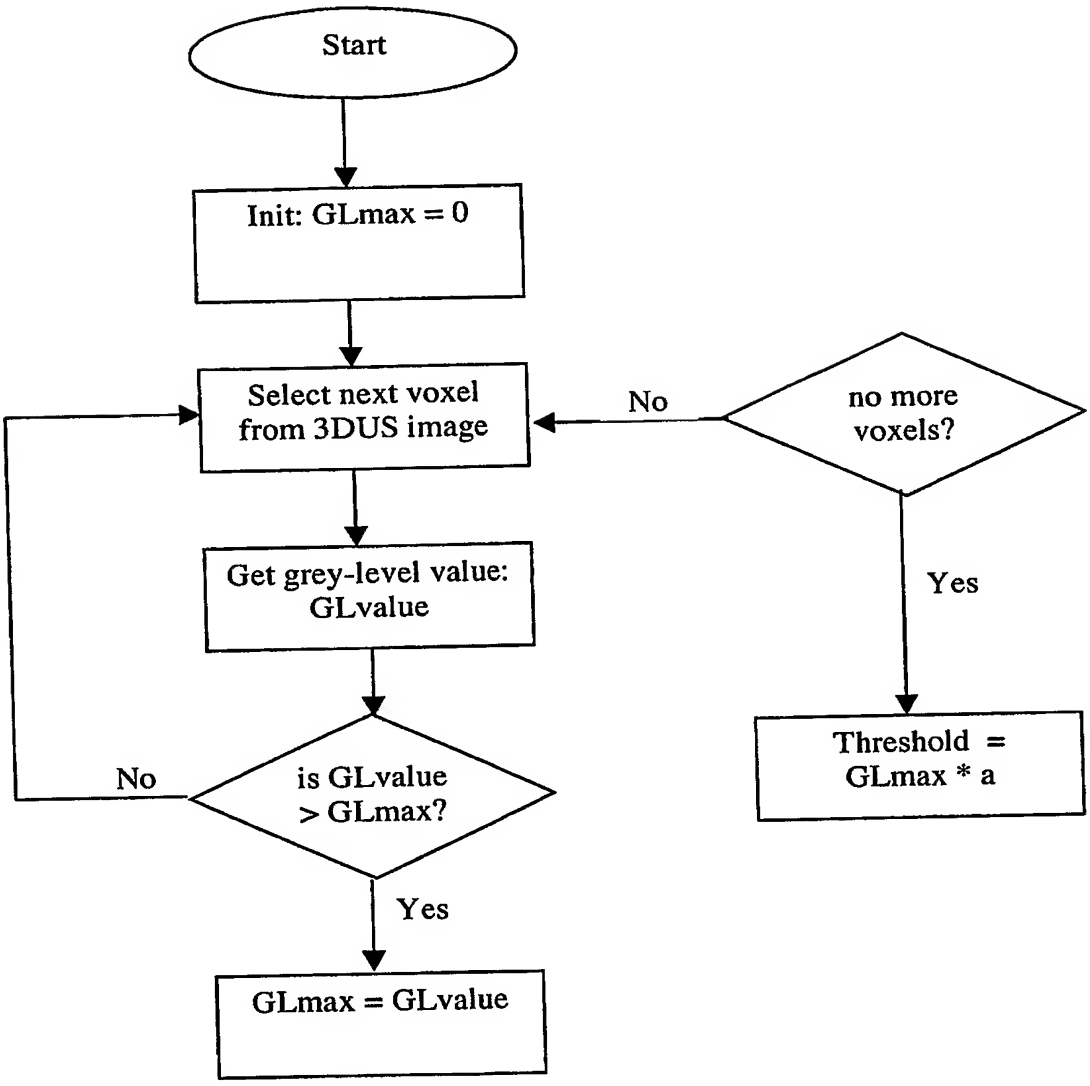


**Figure 6.** Flow chart for calculating the GLC threshold in Block 410 in Fig. 5. Analyze all pixels in the 3DUS post-scan and find the maximum grey-level (GLmax) value. It is assumed that the needle data will have the brightest signal and will generate the highest voxel values in the 3DUS image. The threshold value selected must be less than the maximum grey-level value in the post-scan image. We calculate the threshold value as follows:

Threshold value = GLm * a; where $0 < a < 1$

where optimum value of a is found by experimentation.

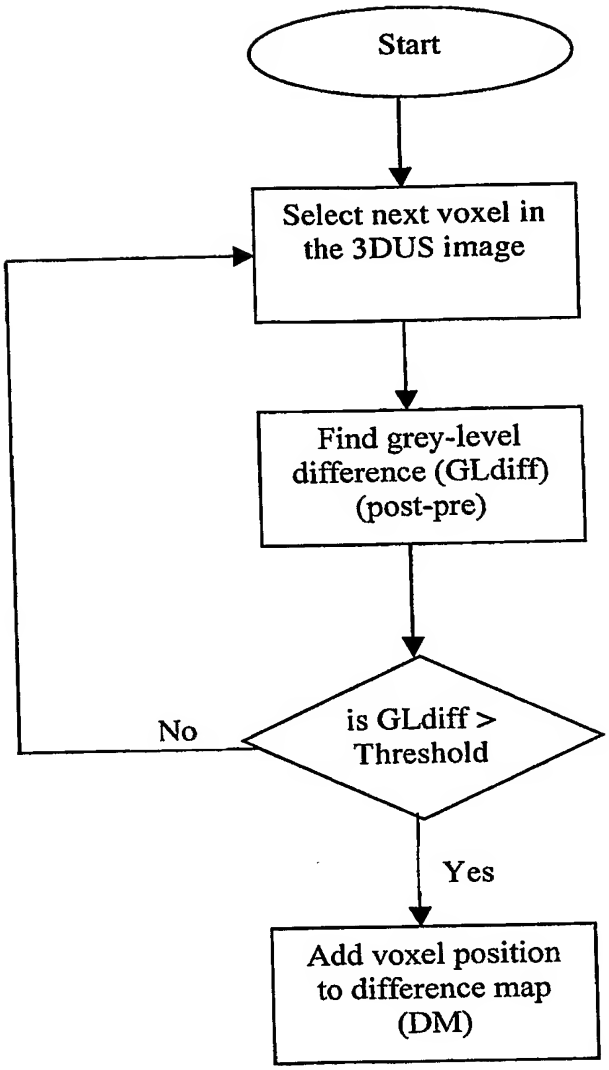


**Figure 7.** Details of Block 420 in Fig. 5. Flow chart for generate the difference map (DM) from the 3D US image. A difference map (DM) is an array of 3D voxel locations (x,y,z) within the 3DUS image where the grey-level difference between pre and post scan exceeds the GLC threshold value. If 2D images are used, then DM is a 2D map.

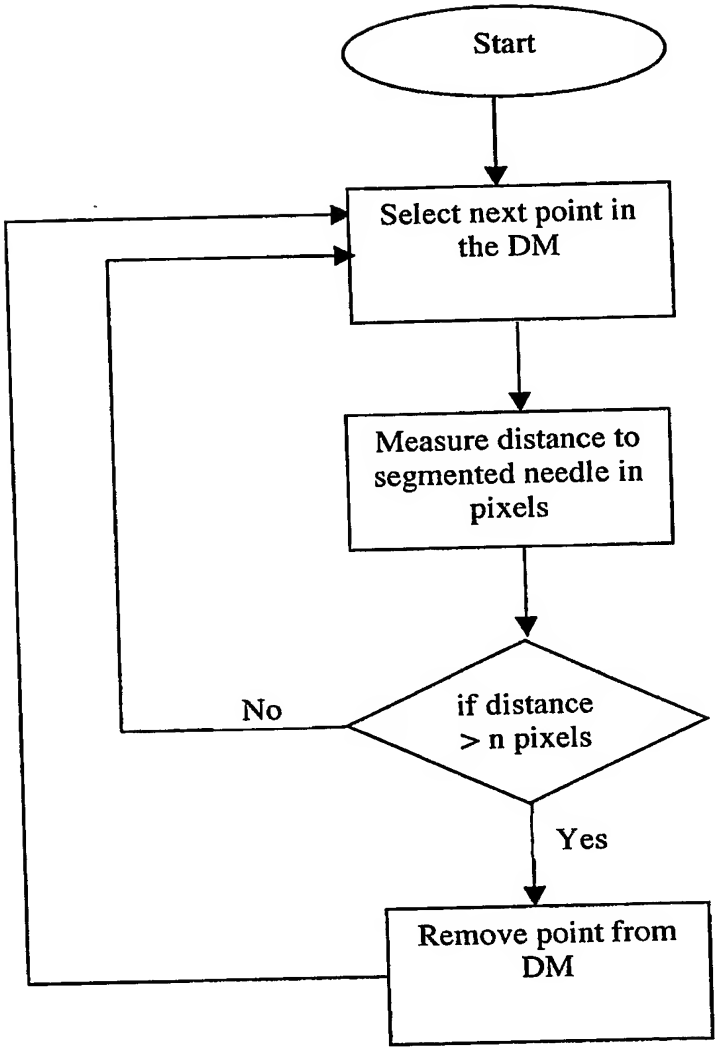


**Figure 8.** Details of Block 460 in Figure 4, in which the Difference Map (DM) is filtered. After determining the trajectory of the needle, we throw away points in the DM that are far away (by n pixels) from the equation of the line defining the needle. We then perform a least squared fit (LSF) on the remaining points in Block 480.

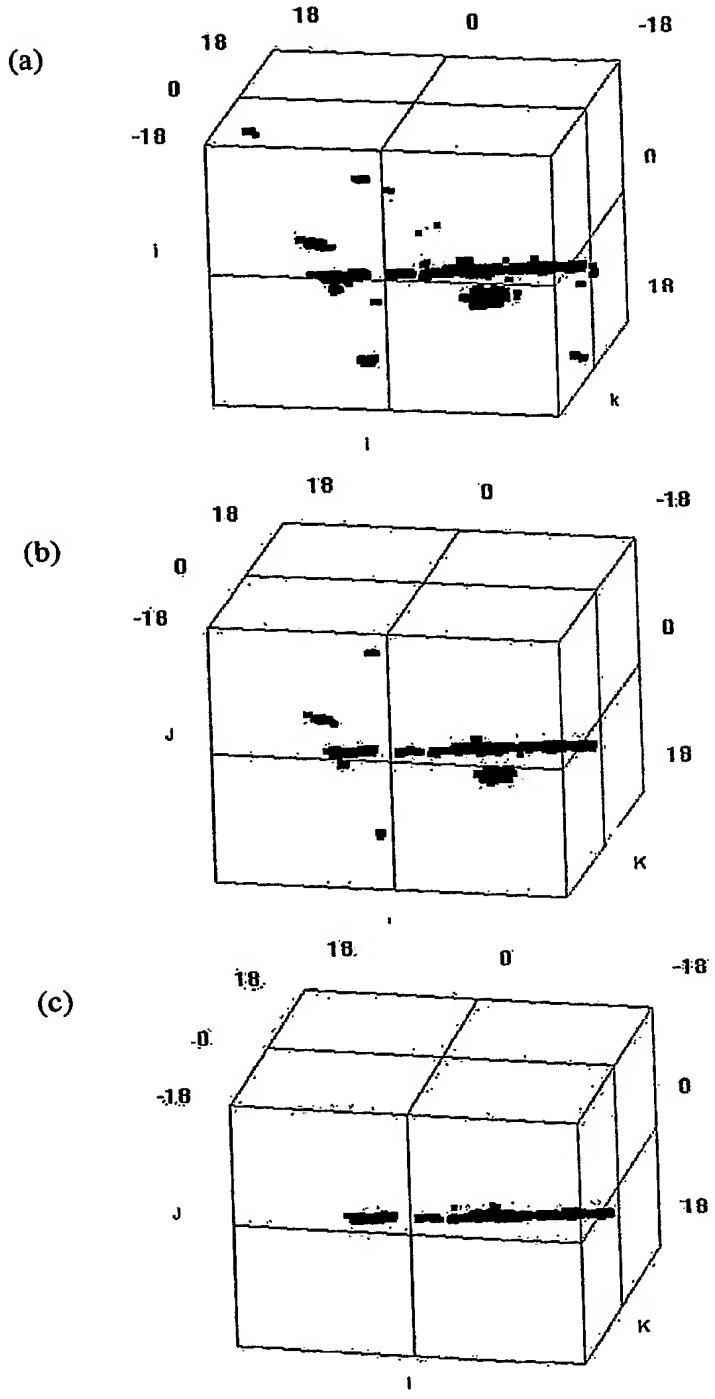


**Figure 9.** Results of the 3D difference map (DM) and processing procedures. (a) 3D difference map (DM) without any processing; (b) the 3D difference map after spurious signals have been rejected; and (c) final 3D difference map (DM) after spurious voxels have been rejected.

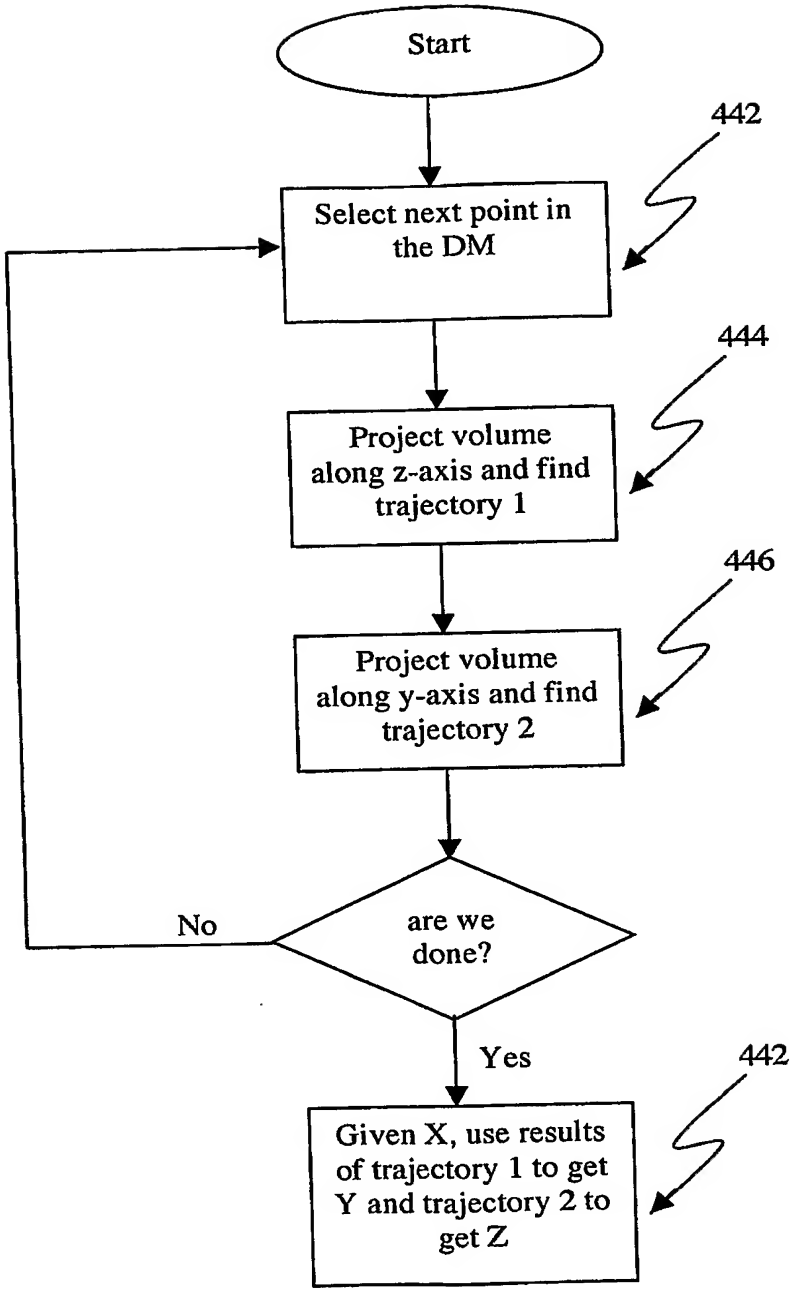


**Figure 10.** Details of Block 480 in Figure 4, in which a least squares fit is performed on the pixels in the DM. The collection of 3D points (x,y,z) referred to as the difference map (DM) contains the voxel positions in the 3DUS image that potentially belong to the set of points defining the needle. To determine the trajectory of the needle, we first apply a 2D least squares fit (LSF) on the x,y component of the voxels in DM. Then, we apply the same 2D LSF to the x,z component of the voxels in DM. The result, are two perpendicular projections of the needle in 2D space, which when combined, give us the trajectory of the needle in 3D space.

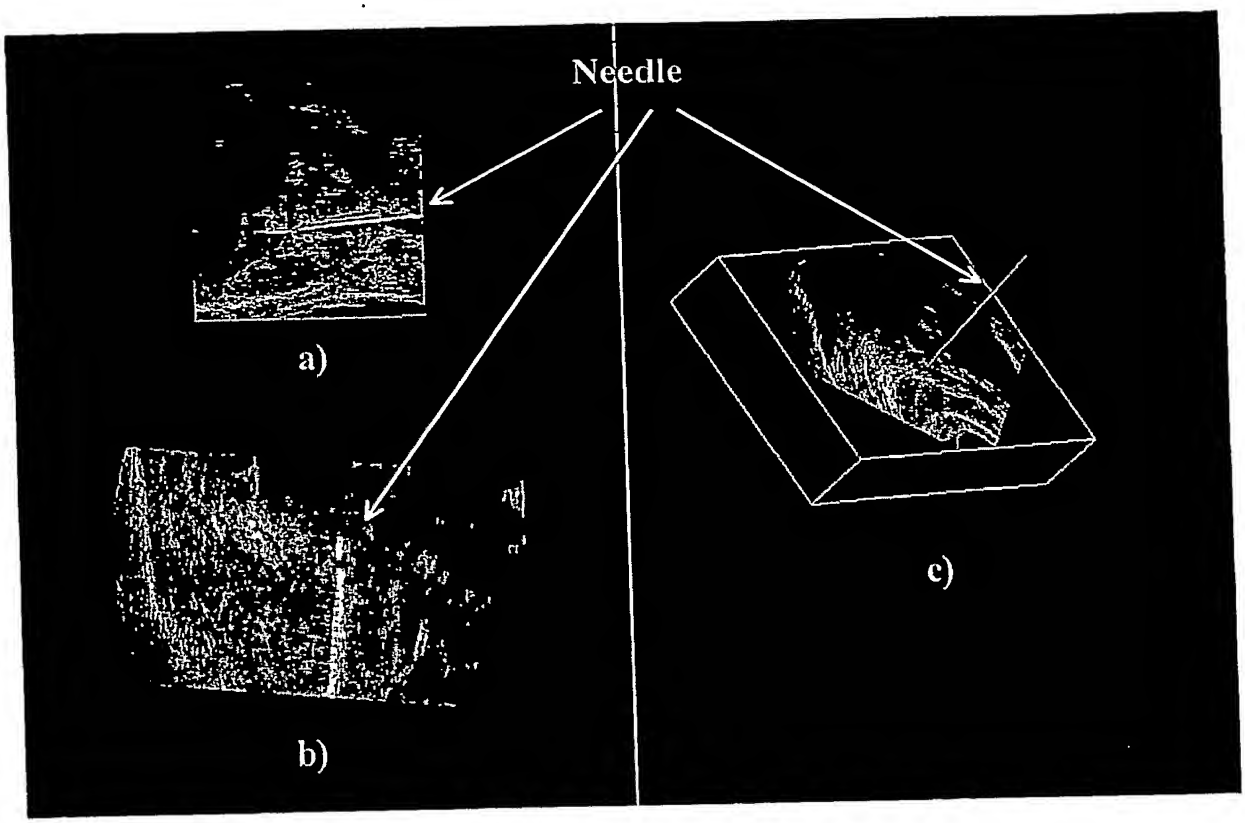


**Figure 11.** Example of Oblique needle segmentation needle tracking obtained during a cryosurgery procedure on a patient's prostate. (a) Oblique sagital view; (b) oblique coronal plane; (c) transverse view with needle projected

**Table 1** Test results for chicken tissue and agar phantoms. 1. Test results for chicken tissue phantom; 2. Test results for agar phantoms.

| | Angle | -15° | -10° | -5° | 5° | 10° | 15° |
|---|---|---|---|---|---|---|---|
| 1 | Time (S) | 0.13 | 0.11 | 0.12 | 0.12 | 0.12 | 0.14 |
| | Accuracy | 0.50° | 0.51° | 0.43° | 0.37° | 0.74° | 0.74° |
| 2 | Time (S) | 0.12 | 0.12 | 0.12 | 0.11 | 0.12 | 0.13 |
| | Accuracy | 0.30° | 0.71° | 0.48° | 0.68° | 0.42° | 0.86° |